

---

# IDENTIFYING TREATMENT EFFECT HETEROGENEITY WITH BAYESIAN HIERARCHICAL ADJUSTABLE RANDOM PARTITION (BHARP) IN ADAPTIVE ENRICHMENT TRIALS

---

A PREPRINT

**Xianglin Zhao**

Department of Epidemiology, Biostatistics, and Occupational Health  
McGill University, Montreal, Quebec, Canada  
xianglin.zhao@mail.mcgill.ca

**Shirin Golchi**

Department of Epidemiology, Biostatistics, and Occupational Health  
McGill University, Montreal, Quebec, Canada

**Jean-Philippe Gouin**

Department of Psychology  
Concordia University, Montreal, Quebec, Canada

**Kaberi Dasgupta**

Department of Medicine  
McGill University, Montreal, Quebec, Canada

August 2025

Preprint. This manuscript has been submitted to *Biometrics* and is currently under review.

## ABSTRACT

Treatment effect heterogeneity refers to the systematic variation in treatment effects across subgroups. There is an increasing need for clinical trials that aim to investigate treatment effect heterogeneity and estimate subgroup-specific responses. While several statistical methods have been proposed to address this problem, existing partitioning-based methods often depend on auxiliary analysis, overlook model uncertainty, or impose inflexible borrowing strength. We propose the Bayesian Hierarchical Adjustable Random Partition (BHARP) model, a self-contained framework that applies a finite mixture model with an unknown number of components to explore the partition space accounting for model uncertainty. The BHARP model jointly estimates subgroup-specific effects and the heterogeneity patterns, and adjusts the borrowing strengths based on within-cluster cohesion without requiring manual calibration. Posterior sampling is performed via a custom reversible-jump Markov chain Monte Carlo sampler tailored to partitioning-based information borrowing in clinical trials. Simulation studies across a range of treatment effect heterogeneity patterns show that the BHARP model achieves better accuracy and precision compared to conventional and advanced methods. We showcase the utilities of the BHARP model in the context of a multi-arm adaptive enrichment trial investigating physical activity interventions in patients with type 2 diabetes.

**Keywords** Bayesian hierarchical model; dynamic information borrowing; finite mixture model; model uncertainty; precision medicine; reversible-jump Markov chain Monte Carlo.

## 1 Introduction

Treatment effect heterogeneity (TEH) refers to the systematic variation in treatment effects across subgroups. In this paper, a “subgroup” refers to a prespecified category of subjects sharing a prognostic covariate profile. For precision medicine aiming to tailor interventions to individual characteristics, understanding the TEH pattern is a key goal, as

such patterns may reveal the underlying biological mechanisms and direct future clinical decisions. However, explaining TEH structures is challenging: the uneven distribution of subgroups may result in loss of power [Freidlin et al., 2010, Rosenblum and Hanley, 2017], and identifying the TEH structure in parallel with effect estimation remains challenging [Xu et al., 2020, Thall, 2021]. Therefore, specialized methods are needed for clinical trials investigating TEH.

Bayesian methods offer a flexible framework to address these challenges. In particular, Bayesian hierarchical models (BHM) [Thall et al., 2003, Berry et al., 2013] borrow information across all subgroups, substantially improving power when response is similar across subgroups [Chen and Lee, 2020, Zheng and Wason, 2022]. However, in the presence of TEH, full exchangeability assumption becomes problematic as it over-shrinks subgroup-specific estimates, biasing the treatment effect estimation and masking the TEH pattern.

Several extensions of BHM have been proposed to mitigate this issue. For example, Chu and Yuan [2018a] empirically calibrate the borrowing strength. Some proposed methods relax full exchangeability assumption via a mixture model [Neuenschwander et al., 2016] or hypothesis-testing [Chen and Lee, 2019, Jiang et al., 2021, Kang et al., 2021]. Specifically, Neuenschwander et al. [2016] combine a pooled distribution with subgroup-specific distributions and Chen and Lee [2019] classify subgroups into responsive and non-responsive clusters and then apply separate BHM within each cluster. However, these methods obscure finer TEH patterns among subgroups. Understanding which subgroups are similar and which ones are not is often more informative, motivating partitioning strategies that explicitly capture TEH structures.

Partitioning-based methods classify subgroups into clusters with similar responses [Zhou and Ji, 2024, Lu and Lee, 2023]. Within each cluster, subgroup-specific parameters are assumed to be exchangeable, enabling information borrowing, while parameters across clusters are treated as nonexchangeable to avoid over-shrinking. This partial exchangeability assumption balances estimation efficiency and the fidelity to the TEH structure. Yet, existing partitioning-based methods face three major limitations.

The first limitation is regarding the exploration of the partition space. Existing approaches either enumerate the entire partition space or select one single “optimal” partition. For example, Psioda et al. [2021] perform Bayesian model averaging across the closed-form posteriors of all possible partitions; Chen and Lee [2020] and Lu and Lee [2023] define an evaluation index and select the partition that maximizes it. However, the number of possible partitions increases exponentially with subgroups (e.g., 115,975 for 10 subgroups), making it impractical to enumerate exhaustively. Moreover, the selection of a single partition is also undermined: different optimization criteria may favor different partitions, and under a certain criterion, multiple partitions often perform similarly.

Many existing methods rely on auxiliary analyses. Some methods require post hoc procedures to obtain an interpretable TEH pattern. For example, the interpretability of Bayesian additive regression trees (BART) requires a single-tree approximation [Logan et al., 2019]. Most partitioning-based hierarchical models [Chen and Lee, 2019, 2020, Lu and Lee, 2023] are constructed based on a preliminary step to determine the structure and strength of information borrowing.

Another common shortcoming of existing approaches stems from inflexible borrowing of information within clusters. Typically, information borrowing is implemented by drawing co-clustering subgroup-specific parameters from a common distribution, whose variance determines the borrowing strength. Some methods apply maximal borrowing with a degenerate distribution [Psioda et al., 2021]. Others tune the borrowing strength based on explicit calculation of cluster cohesion, allowing for limited flexibility. For instance, Chen and Lee [2020] scale pairwise borrowing with co-clustering probabilities, and Lu and Lee [2023] adjust borrowing within clusters with total variation distance.

To address these limitations, we propose the Bayesian Hierarchical Adjustable Random Partition (BHARP) model, an efficient and flexible fully Bayesian framework that identifies TEH structures in parallel with treatment effect estimation. The BHARP model is formulated as a finite mixture model (FMM) with an unknown number of components. It averages over the partition space via sampling to account for uncertainty, directly captures subgroup similarity patterns and automatically adjusts the structure and strengths of information borrowing. We implement a custom reversible-jump Markov chain Monte Carlo (rjMCMC) algorithm to traverse parameter spaces with varying dimensionality, jointly estimating subgroup-specific parameters and latent borrowing structures. Although rjMCMC has been used in other contexts such as variable selection, existing implementations are not applicable to partitioning-based information borrowing. To our knowledge, our implementation is the first application of rjMCMC to dynamic partitioning of heterogeneous treatment effects.

To evaluate the performance of the BHARP model, we conduct simulation studies across a range of TEH scenarios with varying subgroup sizes, balance, and degrees of heterogeneity. We compare the BHARP model against simplified parametric models as well as Bayesian additive regression trees in terms of the accuracy and precision of point estimates. In addition, we embed the BHARP model within Bayesian adaptive trial decision rules: at each interim

analysis, we enable enrichment of responsive subgroups and early termination of interventions where sufficient evidence is available. Finally, we demonstrate the applicability of the method in a real-world multi-arm clinical trial investigating behavioral interventions for patients with type 2 diabetes. Results from trial simulations illustrate that the BHARP model can effectively recover prespecified TEH patterns across intervention arms and support data-driven interim decisions in adaptive trial settings.

The remainder of the paper is organized as follows. Section 2 introduces the BHARP framework, including the model, computation and an adaptive trial design. To compare the proposed method with alternative methods, Section 3 investigates estimation accuracy and precision in a simulation study. Section 4 presents simulations for a hypothetical design scenario inspired by a real-world multi-arm trial. Section 5 follows with a discussion.

## 2 Methodology

### 2.1 Model

Consider a clinical trial comparing  $I$  interventions across  $K$  subgroups, forming  $I \times K$  subgroup-arm cells. Let  $\mathbf{Y}_{ik}$  denote the continuous outcome for subgroup  $k$  receiving intervention  $i$ ,  $i = 1, 2, \dots, I$ ;  $k = 1, 2, \dots, K$ . We assume,

$$\mathbf{Y}_{ik} \sim N(\theta_{ik}, \varsigma^{-1}).$$

We decompose the means as:

$$\theta_{ik} = \beta_i + \Delta_{ik}, \quad \sum_k \Delta_{ik} = 0. \quad (1)$$

For an intervention  $i$ , the arm average  $\beta_i$  represents the overall response level, and  $\Delta_i$  is the deviation from the average response and captures the heterogeneity pattern. The constraint ensures identifiability by centering the TEH structure around the arm averages.

To borrow information between subgroups receiving intervention  $i$ , we assume that  $\Delta_i$  arise from a FMM with an unknown number of mixture component  $q^i \in \{1, \dots, K\}$ . This induces a partitioning structure with subgroup-specific parameters from a common mixture component correspond to a cluster with similar responses. We introduce the vector  $\mathbf{z}^i = (z_1^i, \dots, z_K^i)$  to indicate the component allocation of the  $K$  subgroups. Therefore, we have,

$$\Delta_{ik} | \boldsymbol{\mu}^i, \boldsymbol{\sigma}^i, z_k^i \sim N(\mu_{z_k^i}^i, \sigma_{z_k^i}^i), \quad \mathbf{z}^i | q^i, \mathbf{w}^i \sim \text{Multinomial}(q^i; \mathbf{w}^i). \quad (2)$$

The priors are specified as follows:

$$\begin{aligned} \varsigma &\sim \text{Gam}(a_{\text{cell}}, b_{\text{cell}}), \\ \beta_i &\sim N(c_i, p_i^{-1}), \\ P(q^i) &\propto (q^i)^\alpha, \\ \mathbf{w}^i | q^i &\sim \text{Dirichlet}(1, 1, \dots, 1), \\ \boldsymbol{\sigma}^i | q^i &\sim \text{InvGam}(a_{\text{within}}, b_{\text{within}}), \\ \boldsymbol{\mu}^i | q^i, \tau^i &\sim N(0, (\tau^i)^{-1}), \\ \tau^i &\sim \text{Gam}(a_{\text{between}}, b_{\text{between}}), \end{aligned}$$

where  $\text{Gam}(a, b)$  and  $\text{InvGam}(a, b)$  denote gamma and inverse-gamma distributions with shape parameter  $a$  and rate parameter  $b$ , and  $N(c, p^{-1})$  denotes a normal distribution with mean  $c$  and precision  $p$ . Below we explain the rationale for the choices of prior distributions as well as the specification of hyperparameters.

**Precision**  $\varsigma$  and **arm average**  $\beta_i$  are assigned a Gamma prior and a Normal prior, respectively. These semi-conjugate priors yield closed-form full conditional distributions in the nested Gibbs sampler within rjMCMC (see Supplementary Materials). Compared to the other parameters,  $\varsigma$  and  $\beta_i$  are better-informed by the data, and thus do not require strongly informative hyperparameters. Different hyperparameters may be specified for the average response level in each arm when prior information is available.

For brevity, we omit the intervention index  $i$  in the notation below.

**Allocation vector**  $\mathbf{z}$  assigns each subgroup  $k$  to one of the  $q$  mixture components, with  $z_k = t$  indicating that the response of subgroup  $k$  is generated from component  $t$ . By definition,  $\mathbf{z}$  follows a multinomial distribution conditional on number of components  $q$  and component weight  $\mathbf{w}$ . Therefore, each vector  $\mathbf{z}$  defines a partition of subgroups

$\Omega = \{\Omega_t : \Omega_t \neq \emptyset\}$ , with exchangeability holding within each cluster  $\Omega_t = \{k : z_k = t\}$ . All clusters are mutually exclusive, and their union equals to the set of subgroups  $\{1, \dots, K\}$ .

**Number of mixture components**  $q$  is treated as unknown and updated based on the data, providing further flexibility. We assign a prior of the form  $P(q) \propto q^\alpha$  where  $\alpha = 0$  yields a uniform prior, and larger values of  $\alpha$  encourage models with more mixture components. By definition,  $q$  is upper bounded by the number of subgroups, and sets the *maximum* number of clusters that can be formed. Even when  $q$  is large, all subgroups may still be assigned to the same cluster. Thus, a uniform prior over  $q$  still implicitly favors information borrowing across all subgroups. To prevent over-merging, we recommend higher values of  $\alpha$  to conservatively borrow information and adaptively uncover the TEH structure. Nevertheless, with sufficient data, the posterior distribution of  $q$  and the corresponding number of clusters converge to similar values, reflecting the underlying heterogeneity. Moreover,  $q$  is the dimensionality of component-related parameters  $\mathbf{w}, \boldsymbol{\sigma}, \boldsymbol{\mu}$ , so changing  $q$  leads to transdimensional updates in the parameter space.

**Component weights**  $\mathbf{w}$  are assigned a conjugate Dirichlet prior. Specifically, we apply the symmetric prior  $Dirichlet(1, \dots, 1)$  which does not favor any particular component and is considered weakly informative. While the symmetric prior induces label switching and non-identifiability in component-specific parameters, this does not hinder valid posterior inference. In practice, the algorithm does not rely on component labels. Although we do not assume component means to be ordered, each MCMC chain maintains internally consistent label throughout the sampling. Moreover, our inferential targets, such as co-clustering probabilities, are invariant to label permutations. If prior information suggests substantial distinctions among specific subgroups, asymmetric priors and identifying constraints may be introduced.

**Within-component variances**  $\boldsymbol{\sigma}$  govern the strengths of information borrowing and reflect the cohesion among co-clustering subgroups. To infer the TEH structure from the level of borrowing, it is essential to specify a clinically significant level of heterogeneity. The within-component variances should be small enough if co-clustering is to be interpreted as practical equivalence. Otherwise, the model will simultaneously define and evaluate TEH. To avoid this circular reasoning, we define TEH based on domain knowledge and assign an informative inverse-gamma prior with shape  $a_{\text{within}}$  and rate  $b_{\text{within}}$ , chosen such that most prior density of the mixture component lies around a clinically indistinguishable threshold. Each mixture component is controlled to be narrow enough to generate practically equivalent treatment effects. The informativeness of the prior is calibrated based on expected sample size and effect size. In the presence of sparse data and weak signals, a more concentrated prior is required to enforce tighter cohesion within components.

**Between-component precision**  $\tau$  controls the dispersion of **component means**  $\boldsymbol{\mu}$ . Smaller values of  $\tau$  promote dispersed components, facilitating the identification of distinct treatment effects. However, if  $\tau$  is too small, the component means may be placed unrealistically far from the observed data, leading to incorrect subgroup allocations and excessive shrinkage. Moreover, since this layer is updated based on component centers, the posterior distribution of  $\tau$  may closely resemble its prior, making prior regularization necessary. Therefore, we assign a weakly informative gamma prior with shape  $a_{\text{between}}$  and rate  $b_{\text{between}}$ , which down-weights extreme values of  $\boldsymbol{\mu}$  without being overly informative. This prior helps ensure that the component means remain anchored within a plausible range informed by the data.

Generally, to interpret between-component differences as clinically meaningful, the component means  $\boldsymbol{\mu}$  should be well-separated relative to within-component variances  $\boldsymbol{\sigma}$ . In other words, differences within the same component should be more likely than differences between component means to fall within a clinically negligible range. This principle guides the justification of  $a_{\text{within}}$ ,  $b_{\text{within}}$ ,  $a_{\text{between}}$  and  $b_{\text{between}}$ . We compute the crossover threshold  $\delta$ , defined as the largest value such that the prior density of within-component differences exceeds that of differences between component means over the interval  $(-\delta, \delta)$ . This threshold reflects the minimal heterogeneity level at which two subgroups are more likely to be assigned to different components rather than the same one. By verifying that  $\delta$  does not exceed the clinically significant difference we aim to detect, we ensure that the prior specification supports practically relevant partitions.

## 2.2 Computation

Bayesian inference for the BHARP model is conducted using Markov chain Monte Carlo (MCMC), since the posterior distribution lacks a closed-form expression. Specifically, we employ a rjMCMC algorithm [Green, 1995], an extension of MCMC that enables transitions across parameter spaces with varying dimensionality. The rjMCMC algorithm jointly samples over the partition structure and model parameters, thereby simultaneously capturing posterior uncertainty in both.

The core steps of the algorithm follow the split-merge scheme described by Nobile and Green [2000]. All model parameters are initialized from the prior distribution and are updated based on observed data. Each update iteration

consists of two procedures: the first updates parameter values within the current dimension, while the second proposes a transdimensional move that is accepted with a calculated probability. The first updating procedure is a standard Gibbs sampling step, in which all parameters are drawn from their full conditional distributions, available in closed form.

The ability of rjMCMC to explore models with varying dimensionality arises from the updating procedure with reversible jumps. At each iteration, the algorithm randomly proposes either a “merge” (decreasing the number of components by one) or a “split” (increasing it by one) move. To maintain continuous indexing of components, in a merge move, the last component is absorbed into another randomly selected component; in a split move, a randomly chosen component ejects a new one, appended to the end of the list. The parameters  $w$ ,  $\mu$  and  $\sigma$  of new component(s) are based on auxiliary variables  $u_1$ ,  $u_2$  and  $u_3$  generated from beta distributions (see Supplementary Materials). Specifically, in a split proposal,  $u_1$  controls the allocation of weight between the two resulting components,  $u_2$  determines the offset of the new means from the original center, and  $u_3$  governs the variance split. The merge proposal is constructed as the reverse of a split.

The proposed move is then accepted with a probability that preserves detailed balance. The acceptance probability depends on the likelihood and prior ratios between the proposed and current models, the proposal probabilities of the forward and reverse moves, and the determinant of the Jacobian matrix corresponding to the parameter transformation. If accepted, the Markov chain transitions to a new model dimension; otherwise, the chain remains in the current state.

In low-signal settings, the default rjMCMC algorithm tends to fit simpler models with large incoherent clusters. Therefore, we introduce modifications tailored to clinical trials where the number of subgroups may be small and heterogeneity may be subtle. For the number of components  $q$ , we employ an informative prior  $P(q) \propto q^2$  in favor of finely partitioned clusters with conservative information borrowing. The frequency of split moves is increased from the default 0.5 to 0.6, offsetting the tendency to merge clusters. In addition, the distributions of auxiliary variables  $u_1$ ,  $u_2$  and  $u_3$  are more concentrated to prevent unrealistic extreme separation, thereby improving the proposal quality and acceptance rate. These modifications encourage the sampler to explore complex models with higher parameter dimensions.

The algorithm is implemented in C++ using the Rcpp interface, providing efficiency for the compute-intensive rjMCMC sampling. Our rjMCMC implementation is the first one to address dynamic partitioning, as existing ones are primarily designed for variable selection. The algorithm is wrapped as a user-friendly R function to integrate into standard statistical analysis workflows. Further details are provided in the Supplementary Materials.

### 2.3 Adaptive Design

In this section, we describe an adaptive enrichment trial design that modifies the enrollment criteria to focus on responsive subgroups and allows for early termination of treatment arms once sufficient evidence is accumulated. Decisions are based on the posterior distribution of  $\theta_{ik}$ , i.e., the expected response of subgroup  $k$  to intervention  $i$ , conditional on data  $\mathcal{D}_\ell$  up to analysis  $\ell = 1, 2, \dots, \mathcal{L}$ , where  $\mathcal{L}$  denotes the final analysis. The decisions rely on clinically meaningful boundaries for efficacy and futility ( $x_E$  and  $x_F$ , respectively) along with posterior probability decision thresholds ( $\mathcal{P}_{\ell,E}$  and  $\mathcal{P}_{\ell,F}$ ). These thresholds may be set more stringently at early analyses to mitigate the impact of early-stage sampling variability.

At each interim analysis  $\ell = 1, \dots, \mathcal{L} - 1$  the following sequential procedures are applied: **Enrichment:** Conclude futility and deactivate recruitment of subgroup  $k$  in arm  $i$  if  $P(\theta_{ik} \leq x_F | \mathcal{D}_\ell) > \mathcal{P}_{\ell,F}$ ; **Efficacy:** For interventions remaining active in at least one subgroup, test the efficacy hypothesis in each active cell  $(i, k)$ . Conclude efficacy if  $P(\theta_{ik} > x_E | \mathcal{D}_\ell) > \mathcal{P}_{\ell,E}$ ; **Arm termination:** Cease randomization to intervention  $i$  if all associated subgroups have reached any conclusion. **Continued Accrual:** If the trial continues beyond interim analysis  $\ell$ , recruitment continues for all unresolved subgroup-arm combinations until the next analysis  $\ell + 1$ . At the final analysis  $\ell = \mathcal{L}$ , for each unresolved subgroup-arm combinations, conclude futility if  $P(\theta_{ik} > x_F | \mathcal{D}_\mathcal{L}) > \mathcal{P}_{\mathcal{L},F}$  and conclude efficacy if  $P(\theta_{ik} > x_E | \mathcal{D}_\mathcal{L}) > \mathcal{P}_{\mathcal{L},E}$ .

The adaptive decision framework is guided by three primary considerations: early identification and deactivation of futile subgroups enables the enrichment of promising subgroups in later trial stages; accrual continues in subgroups demonstrating efficacy until sufficient evidence is collected for the entire intervention arm, as premature discontinuation of access to potentially beneficial treatments during ongoing evaluation raises ethical concerns; and the design allocates resources across arms with different TEH complexity. Interventions with simpler TEH structures (e.g., homogeneity or readily identifiable heterogeneity) benefit more from dynamic information borrowing and reach conclusions faster. This enables early termination of such arms and reallocation of sample size to arms with more complex TEH structures that require additional data to identify.

### 3 Simulation Study

In this section, we compare the BHARP model with parametric models with simplified structure as well as a flexible non-parametric model in simulation studies assessing the accuracy and precision of point estimates in a non-comparative analysis across diverse TEH scenarios.

#### 3.1 Comparator Methods

To assess the contribution of each element in the proposed BHARP framework, we compare it with the following alternative methods: a Bayesian independent (IND) model, a basic BHM [Berry et al., 2013] and an FMM with fixed number of components (BLAST) [Chu and Yuan, 2018b]. Each comparator is derived by excluding specific elements from the BHARP model, thereby highlighting the contribution of each element. All methods share common hyperparameter settings wherever applicable. Additionally, to benchmark against a flexible yet less interpretable non-parametric method, we include Bayesian additive regression trees (BART) [Chipman et al., 2010]. Detailed model specifications are given below.

**IND:** This model treats each subgroup-arm cell as an independent sub-trial without borrowing information. The response in cell  $(i, k)$  is modeled as  $\theta_{ik} \sim N(c_{ik,IND}, p_{ik,IND}^{-1})$  updated solely with  $\mathbf{Y}_{ik}$ . The hyperparameters  $c_{ik,IND}$  and  $p_{ik,IND}$ , are matched to  $c_i, p_i$  in BHARP model. This no-borrowing model serves as a benchmark.

**BHM:** A standard BHM is applied within each intervention arm, assuming full exchangeability across subgroups. The subgroup-specific parameters follow  $\theta_{ik} \sim N(\beta_{i,BHM}, \tau_{i,BHM}^{-1})$ , with priors for  $\beta_{i,BHM}, \tau_{i,BHM}$  matched to those of  $\beta_i, \tau^i$  in the BHARP model. Conceptually, this model excludes the partitioning FMM layer from the BHARP model. While both the BHM and the BHARP model include a weak-borrowing layer, a distinction lies in the unit of shrinkage: the BHM performs subgroup-level updates, whereas the BHARP model applies shrinkage at the component level, involving fewer units than subgroup levels. Furthermore, the purpose of the weak-borrowing layer is different: it serves as the primary mechanism of information sharing in the BHM, but contributes only marginally in the BHARP model, where primary borrowing occurs through the partition structure.

**BLAST:** This method is based on the same FMM as the BHARP model. The only difference is it assumes that the component number  $q$  to be fixed. Rather than assigning a prior to  $q$ , its value is selected from 1, 2, 3 based on the deviance information criterion. Comparing with the BLAST method allows us to investigate the added flexibility in the BHARP model by unknown number of components. To make the results comparable, we modify the original BLAST model to have identical hyperparameters and likelihood as the BHARP model.

**BART:** This method uses sum of shallow regression trees to flexibly learn the relationship between covariates and response. In BART, the subgroup indicators are treated as categorical covariates. We implement BART using the BART package in R with default settings.

In the simulation study, methods are compared over 500 simulated data sets under each scenario using parallel computing. For each data set, inference for the parametric models is made using four MCMC chains with 2,000 iterations each. The posterior median is used as the point estimator. BART is implemented with a single chain due to the lack of built-in multi-chain support in the BART package and the considerable computational cost, and additional chains are unlikely to change the conclusions.

#### 3.2 Hyperparameter Specification

In this subsection, we specify hyperparameters  $a_{cell}, b_{cell}, c_i, p_i, a_{between}, b_{between}, a_{within}$  and  $b_{within}$  in the simulation study. These values are chosen for standardized data (following a normal distribution with unit variance) and calibrated with 95% highest density interval (HDI) on interpretable parameter scales (e.g., precision parameters transformed to standard deviation).

The prior for cell-level precision  $\varsigma$  is specified as  $InvGam(a_{cell}, b_{cell}) = InvGam(5, 6)$ , yielding a standard deviation with mode 1 and 95% HDI of (0.71, 1.79), allowing sufficient flexibility in subgroup-level variation. The prior for the  $\beta_i$  parameters (arm average) is  $N(c_i, p_i^{-1}) = N(0, 2^{-1})$ , with a 95% HDI of (-1.39, 1.39), and that of between-component precision  $\tau^i$  is  $Gam(a_{between}, b_{between}) = Gam(4, 4)$ , yielding a standard deviation with mode 0.89 and 95% HDI of (0.61, 1.75). These priors are sufficiently vague to accommodate a wide range of plausible effect sizes.

We fix the mode of standard deviation of components at 0.1, align with the clinically negligible difference in effect sizes. The degree of informativeness depends on the sample size: in the simulations where the minimum subgroup size is 35, we specify  $a_{within} = 70, b_{within} = 0.71$ ; under the choices of  $a_{between}, b_{between}, a_{within}$  and  $b_{within}$ , the crossover value

is approximately 0.31, which remains below the difference between adjacent response levels in data-generating model. This alignment with the TEH assumption ensures the prior supports meaningful and clinically relevant partitions.

### 3.3 Simulation Scenarios

To capture a wide range of TEH structures, we design 9 scenarios as listed in Table 1. All outcomes are generated from normal distributions with unit variance,  $Y_k \sim N(\theta_k, 1)$ , and the true effect sizes take one of three values: low ( $\theta_k = 0$ ), medium ( $\theta_k = 0.65$ ) and high ( $\theta_k = 1.3$ ). Scenarios with the same subgroup counts and absolute differences are considered equivalent. For instance, scenarios such as “7 low, 3 medium”, “7 high, 3 medium” and so on all reflect equivalent TEH structures. We present the scenarios with the least responsive subgroups, as the conservative scenarios more closely reflect the practical challenges of detecting heterogeneous signals in real-world settings.

Table 1: Simulation scenarios of treatment effect heterogeneity with 10 subgroups, where outcomes follow  $Y_k \sim N(\theta_k, 1)$

Scenario	Low ( $\theta_k = 0$ )		Medium ( $\theta_k = 0.65$ )		High ( $\theta_k = 1.3$ )	
	Number	Size	Number	Size	Number	Size
<b>1</b>	10	35	0	–	0	–
<b>2</b>	7	35	0	–	3	35
<b>3</b>	7	35	3	35	0	–
<b>4</b>	7	35	3	70	0	–
<b>5</b>	5	35	5	35	0	–
<b>6</b>	4	35	3	35	3	35
<b>7</b>	4	42	3	84	3	56
<b>8</b>	7	35	2	35	1	35
<b>9</b>	7	35	2	70	1	84

### 3.4 Simulation Results

To compare the performance in estimating subgroup-specific treatment effects, we assess three metrics: root mean squared error (RMSE), mean absolute error (MAE), and the empirical variance of point estimates across simulations. Additional convergence diagnostics for the rjMCMC algorithm are reported in the Supplementary Materials.

Figure 1 presents the RMSE of the evaluated methods across nine scenarios. The true effect sizes are indicated by background shading. Overall, the BHARP model consistently achieves the lowest or second lowest RMSE across most scenarios. It accurately identifies the underlying TEH structure when subgroups are highly homogeneous (Scenario 1) or exhibit pronounced differences (Scenario 2). The challenging scenarios are those with a small number of subgroups differing modestly from neighboring effect size levels, such as in Scenarios 3, 6, and 8. In these cases, the small clusters tend to be over-merged with adjacent ones due to limited information to support complex models. As a result, for the rare subgroups, the efficiency of information borrowing decreases.

The challenge in separating clusters under the scenarios where a small number of subgroups exhibit moderate heterogeneity is less pronounced with more balanced subgroup distributions or increased sample sizes. For instance, compared to Scenario 3, which yields an average co-clustering probability of 0.28 among heterogeneous subgroup pairs, this value decreases to 0.22 in Scenario 5, where the moderate-effect subgroups are more evenly distributed. On the other hand, Scenario 4 assigns larger sample sizes to the rare subgroups compared to Scenario 3, further reducing the co-clustering probability to 0.14. In more complex settings involving three small clusters with minimal separation (Scenario 6), moderate-effect subgroups are often absorbed into adjacent clusters, resulting in a misclassification rate of 0.27. Increasing the overall sample size (Scenario 7) substantially improves performance, lowering the misclassification rate to 0.11 and reducing RMSE accordingly. These results illustrate that cluster separability is influenced by the underlying TEH structure, particularly the balance and size of subgroups exhibiting heterogeneous effects.

The performance of the BHM closely resembles that of the IND model, indicating that the between-cluster layer in the BHARP model contributes only trivial information borrowing. Notably, both FMM-based methods (BHARP and BLAST) differ substantially from the others, underscoring the contribution of partitioning layer in treatment effect estimation. In addition to its improvement in information borrowing, the BHARP model also achieves competitive computational efficiency. Across the nine simulated scenarios (500 replicates each, under identical parallel computing setup on the same laptop), the BHARP model runs faster than the BHM in five scenarios, saving up to 19 minutes in

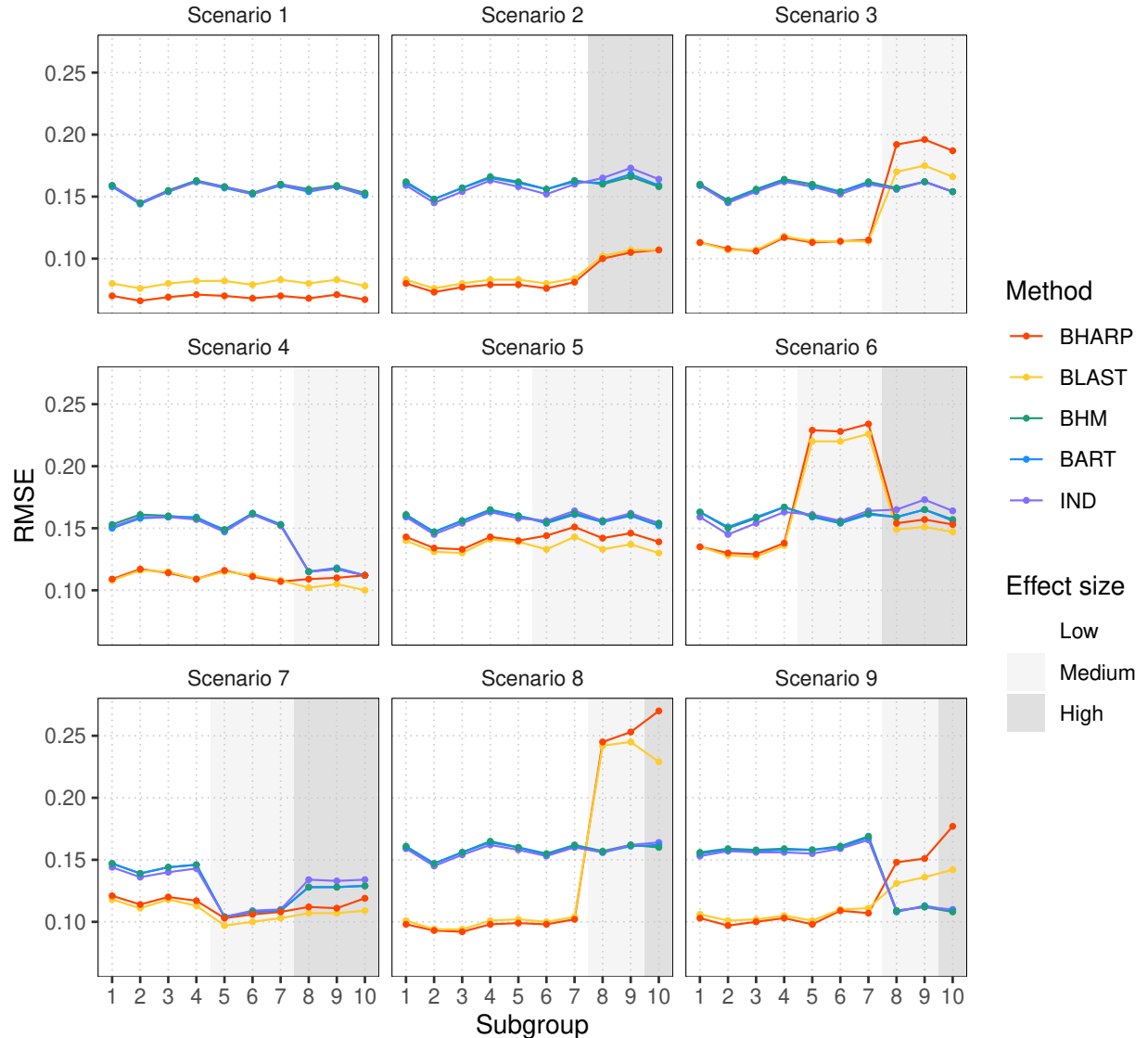


Figure 1: Root mean squared error (RMSE) of posterior median estimates of the BHARP model comparing with the BLAST, BHM, BART, and IND methods in nine scenarios. Gray shading indicates true effect sizes of subgroups. Scenarios 4,7,9 contain increased sample sizes.

Table 2: Definition of patient subgroups.

Subgroup	Marital Quality	Concordance for Excess Weight
1	Low	No
2	Medium	No
3	High	No
4	Low	Yes
5	Medium	Yes
6	High	Yes

some cases. These gains are particularly noteworthy given that the BHARP model both identifies the partition structure and improves the efficiency to estimate subgroup-specific parameters.

The comparison against the BLAST method highlights the negligible loss associated with treating the number of mixture components as an unknown parameter in the BHARP model. Although the BHARP model may not achieve the lowest RMSE for a few subgroups under certain conditions, this trade-off yields substantial gains in interpretability, flexibility, and computational efficiency. First, fixing the number of components can lead to model misspecification and reduced interpretability. When the true subgroup structure is homogeneous, imposing a fixed number of components may result in spurious heterogeneity, as the model attempts to partition the data even in the absence of meaningful differences. Additionally, the true TEH structure is typically unknown in advance, and the choice of component number is often difficult to justify. In contrast, the BHARP model places a prior directly on the partition space and allows the number of components to adaptively reflect the observed data, enabling more interpretable TEH structures across subgroups. Second, fixed-component approaches are inherently less flexible, especially in multi-arm trial settings. BLAST selects the number of components separately for each arm by fitting multiple FMMs with one, two, or three components. While this is tractable for single-arm trials, extending to multi-arm designs quickly becomes computationally burdensome: for  $I$  intervention arms, a total of  $3^I$  models need to be fitted. Alternatively, one could assume a common component number across all arms, which is a rarely justifiable constraint. Finally, the BLAST method typically incurs higher computational cost due to repeated model fitting. In contrast, since the BHARP model jointly estimates the number of components with an efficient algorithm, it is more efficient than BLAST. The total runtime of BLAST ranges from 26 to 42 minutes, while that of BHARP model ranges from 12 to 25 minutes.

Although BART is a flexible nonparametric method, its performance under default settings closely resembles that of IND, showing limited efficiency in information borrowing. BART incurs substantial computational cost due to two factors: the iterative updating of an ensemble of simple trees, and generating posterior predictive distributions at the individual level. The latter requires evaluating the sum of trees for every individual at each MCMC iteration, resulting in high computational burden when the sample size is large. In our simulation, despite generating fewer MCMC samples, BART took up to 78 minutes in a scenario—the longest runtime observed among all methods and scenarios. Lastly, due to its additive tree structure, BART does not directly provide inference on subgroup partition. To obtain an interpretable TEH structure, additional post hoc analysis is necessary, further complicating its application in subgroup-based TEH detection.

MAE results are summarized in Figure 2 and variances of point estimates are reported in Figure 3. These results exhibit trends consistent with those observed in RMSE. Overall, the three evaluation metrics consistently highlight the advantages of BHARP model in accurately and efficiently capturing subgroup-specific treatment effects across diverse scenarios.

## 4 Application to the Partner Step T2D Clinical Trial

We illustrate the application of BHARP framework using a design inspired by the “Partner Step T2D” trial, which evaluates behavioral interventions to increase the step counts among adults with type 2 diabetes (T2D) and their partners. In the actual trial, couples receive wearable step counters and either weekly step targets alone or targets plus a couple-based behavioral coaching (“dyadic coping”) intervention.

While the actual trial involves two intervention arms, for illustrative purposes we consider a three-arm design to showcase BHARP framework’s ability to capture distinct TEH patterns. We simulate an adaptive enrichment design by adding an arm with step counters only (no step targets, no dyadic coping). TEH patterns are assumed to depend on two baseline factors: relationship quality (low/medium/high) and concordance for excess weight (yes/no, defined as both partners having body mass index  $\geq 30 \text{ kg/m}^2$ ). Crossing these factors yields six subgroups (Table 2) that represent distinct patient profiles potentially influencing the treatment effects of three investigated interventions.

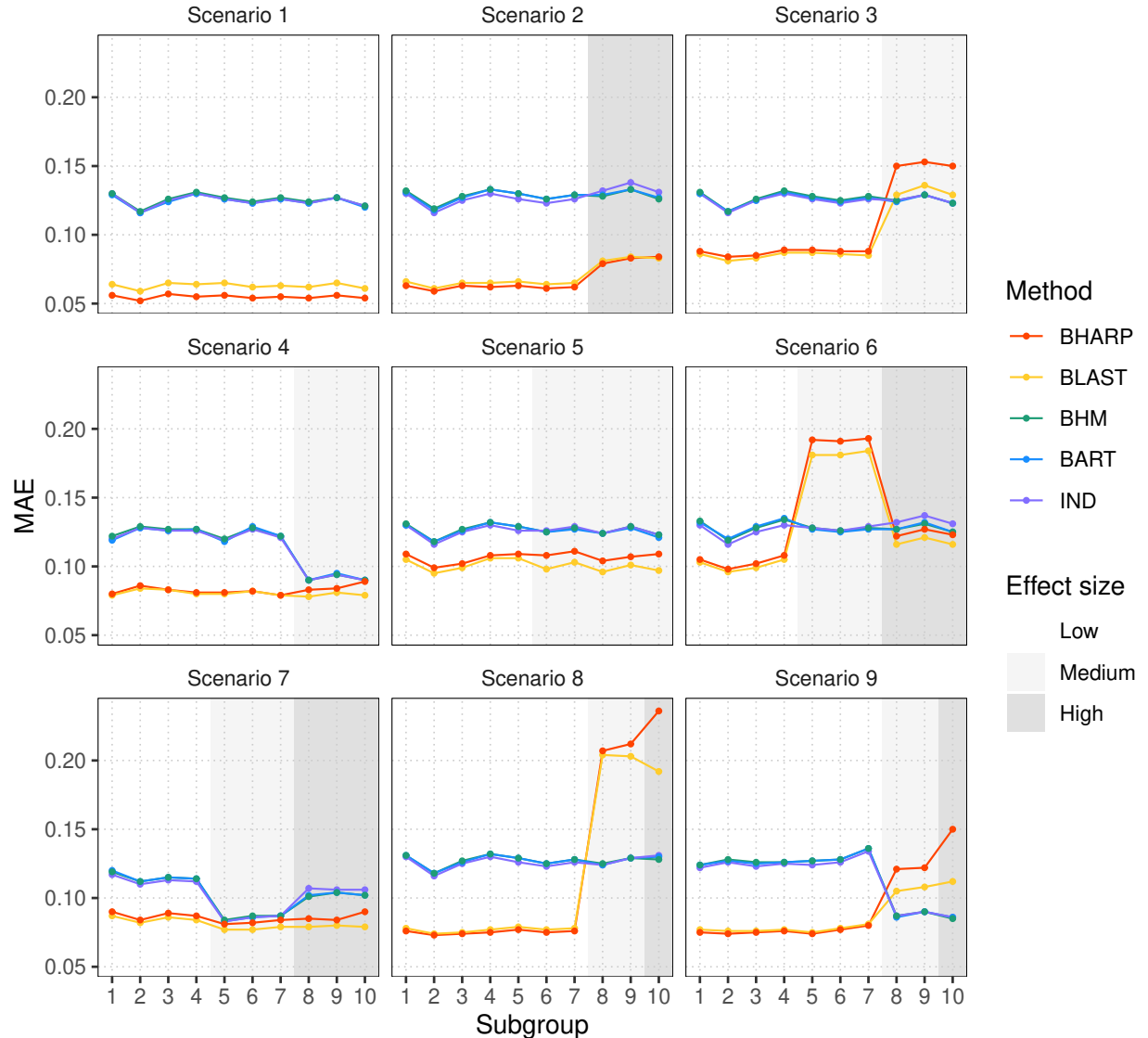


Figure 2: Mean absolute error (MAE) of posterior median estimates of BHARP model comparing with BLAST, BHM, BART, and IND in nine scenarios. Gray shading indicates true effect sizes of subgroups. Scenarios 4,7,9 contain increased sample size.

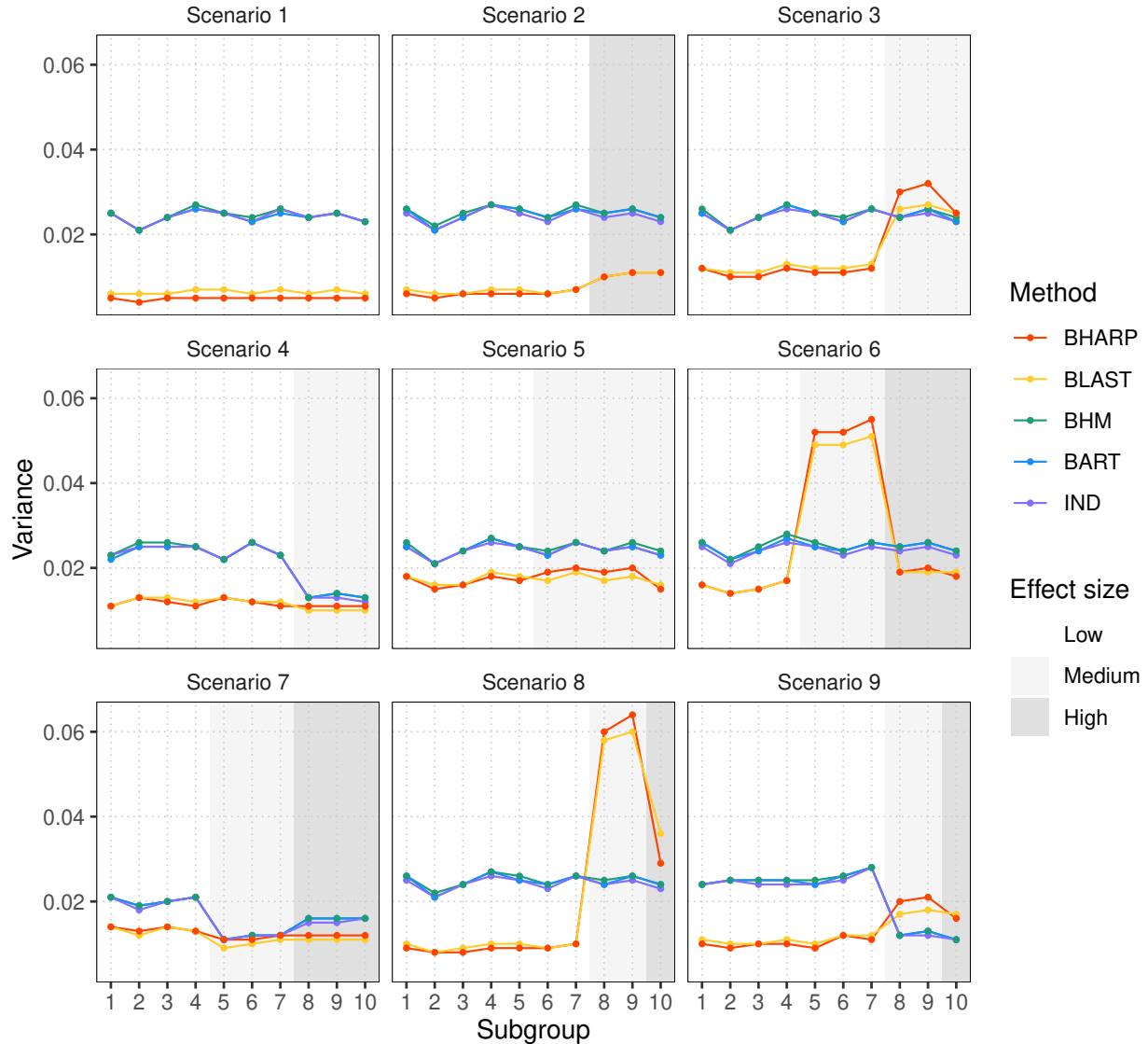


Figure 3: Variance of posterior median estimates of BHARP model comparing with BLAST, BHM, BART, and IND in nine scenarios. Gray shading indicates true effect sizes of subgroups. Scenarios 4,7,9 contain increased sample size.

Table 3: Data-generating  $\theta_{ik}$  for each arm ( $i$ ) and subgroup ( $k$ ), with outcomes independently generated as  $Y_{ik} \sim \mathcal{N}(\theta_{ik}, 1)$ .

Subgroup	1	2	3	4	5	6
Arm 1	0.30	0.30	0.30	0.30	0.30	0.30
Arm 2	-0.05	0.30	0.65	-0.05	0.35	0.65
Arm 3	-0.05	0.00	0.05	0.60	0.65	0.55

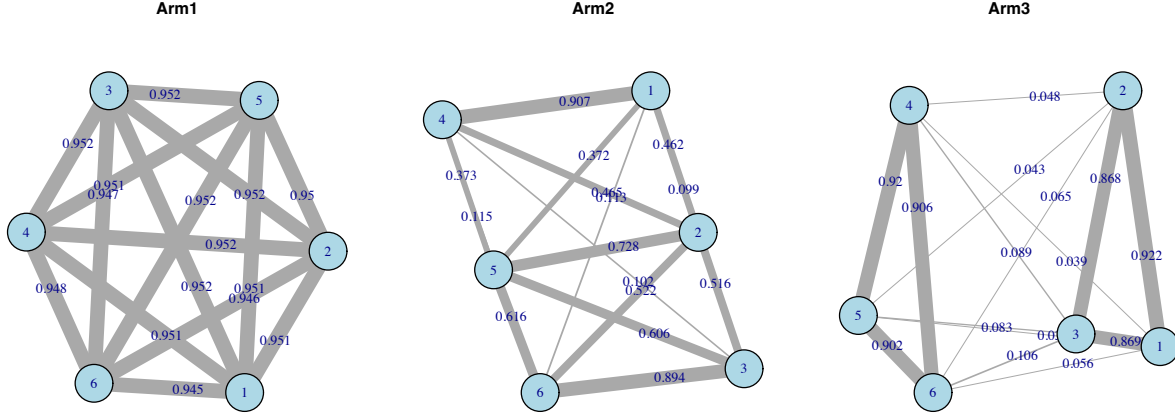


Figure 4: Average co-clustering probabilities estimated by BHARP model. Each panel shows one arm, with nodes for subgroups and edge thickness representing the posterior co-clustering probability. The estimated patterns recover the true partitions:  $\{1, 2, 3, 4, 5, 6\}$  in arm 1,  $\{1, 4\}, \{2, 5\}, \{3, 6\}$  in arm 2, and  $\{1, 2, 3\}, \{4, 5, 6\}$  in arm 3.

The simulation scenarios are constructed to represent, respectively: homogeneous effects (Arm 1), gradient effects aligned with marital quality (Arm 2), and effects concentrated among couples concordant for excess weight (Arm 3). Table 3 presents the subgroup-specific means  $\theta_{ik}$  for each arm, with outcomes generated from  $Y_{ik} \sim \mathcal{N}(\theta_{ik}, 1)$ . Arm 1 exhibits a constant effect of 0.30 across all subgroups, representing a homogeneous scenario with moderate effects. Arm 2 includes three weakly separated response levels, with near-zero responses for subgroups 1 and 4, moderate effects for subgroups 2 and 5, and high responses of subgroups 3 and 6. In Arm 3, subgroups 4, 5 and 6 exhibit responses between 0.55 and 0.65, while subgroups 1, 2, and 3 have near-zero effects.

In the following we describe a hypothetical adaptive enrichment design together with the BHARP analysis model. Interim analyses planned at cumulative sample sizes of 900, 1200, and 1500, with a final analysis at 1800. Evaluation metrics include global false positive rate, generalized power (the probability that at least one effective intervention is correctly identified for every subgroup), arm-specific false negative rates, expected sample sizes, and the RMSE of point estimates. Hyperparameter settings follow those in Section 3.2, except for the within-component variance, for which we specify a less informative prior ( $a_{\text{within}} = 30$ ,  $b_{\text{within}} = 0.31$ ) due to the larger sample size.

We first showcase the utilities of BHARP framework in the analysis of the data and interpretation of the results by presenting the average results of 500 simulated trials under a single scenario where the true TEH structures are as follows:  $\{1, \dots, 6\}$  for Arm 1;  $\{1, 4\}, \{2, 5\}, \{3, 6\}$  for Arm 2; and  $\{1, 2, 3\}, \{4, 5, 6\}$  for Arm 3. Pairwise homogeneity, can be evaluated with co-clustering probabilities, as visualized in Figure 4, where edge widths indicate the average posterior probability of each subgroup pair being partitioned together. Although distinguishing rare and weakly separated subgroups (e.g., in Arm 2) remains challenging, BHARP model generally recovers the underlying TEH structure with high fidelity. Beyond pairwise relationships, BHARP model also supports a more detailed investigation. For example, the probability that subgroups 1 and 2 are equivalent but distinct from subgroup 3. Unlike other existing methods, such probabilities can be directly computed from the posterior samples without additional modeling or post hoc analysis.

Table 4 summarizes the operating characteristics. All methods from Section 3.1 are included for comparison, except for BLAST, which is infeasible in the multi-arm setting due to the exponential growth in analysis complexity. BHARP model is the only method that simultaneously maintains a global false positive rate below 0.05 and achieves a generalized power exceeding 0.95. It also terminates Arm 1 early as expected resulting in smaller expected sample sizes,

Table 4: Comparison of operating characteristics across BHARP, BHM, BART and IND

	<b>BHARP</b>	<b>BHM</b>	<b>BART</b>	<b>IND</b>	
<b>False positive rate (global)</b>	0.036	0.132	0.072	0.112	
<b>Generalized power</b>	0.988	0.892	0.888	0.868	
<b>False negative rate</b>	<b>Arm 1</b>	0	0.036	0.036	0.096
	<b>Arm 2</b>	0.096	0.024	0.024	0.036
	<b>Arm 3</b>	0	0	0	0
<b>Expected sample size</b>	<b>Arm 1</b>	432	669	684	684
	<b>Arm 2</b>	646	521	502	524
	<b>Arm 3</b>	637	569	588	573

*Note.* Generalized power is defined as the probability that, for every subgroup, at least one truly effective intervention is correctly identified.

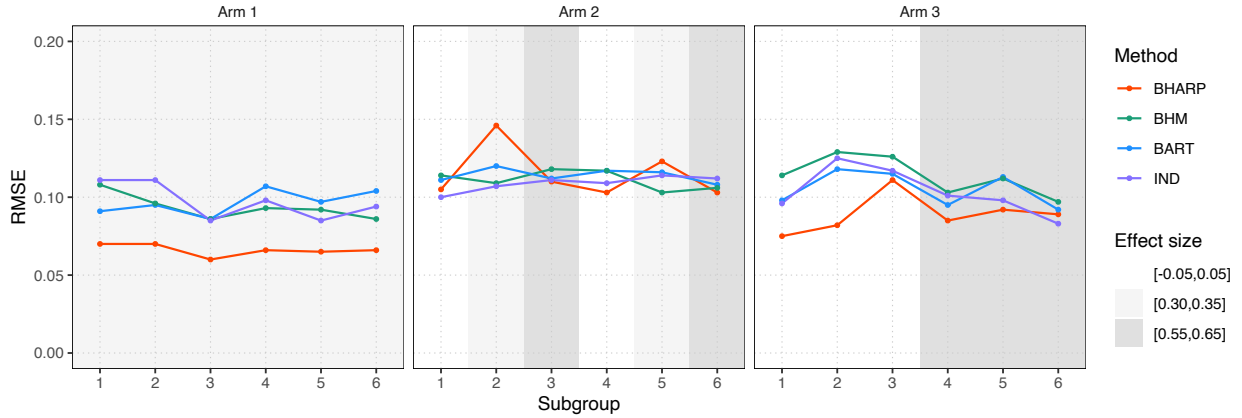


Figure 5: RMSE performance of point estimations provided by BHARP model and comparing methods. Shaded regions indicate the underlying effect size levels.

without incurring false negatives. Figure 5 presents the RMSE comparison across methods in the Partner Step T2D trial. BHARP method achieves consistently low RMSE in most subgroups across arms, reflecting its ability to support adaptive decisions.

## 5 Discussion

In this paper, we proposed the BHARP model, a self-contained Bayesian framework for identifying the TEH structure and adaptively borrowing information to estimate subgroup-specific responses. The proposed approach improves the effectiveness of information borrowing by jointly addressing two key challenges: determining which subgroups are sufficiently similar and adjusting the strengths of borrowing accordingly. By integrating model uncertainty into the exploration of the partition space, the BHARP model provides a coherent and interpretable summary of underlying TEH structures. Furthermore, we provided an efficient and user-friendly implementation of rjMCMC and proposed a trial design embedding the proposed model into the interim decisions of adaptive enrichment trials.

The proposed approach dynamically partitions subgroups through a hierarchical model, in which the partitioning layer—a FMM with an unknown number of components—contributes most to the performance. In our simulation studies, the BHARP model achieved low RMSE for most subgroup-specific estimates, particularly when the heterogeneous response levels were either well-separated or contained a balanced number of subgroups. Compared to existing methods, BHARP model offered comparable efficiency to BHM, greater interpretability than BART, and improved flexibility over FMM with a fixed number of components. In the real-world application to a multi-arm adaptive trial, the BHARP method successfully revealed the TEH structure for all investigated interventions. Meanwhile, it demonstrated desirable operating characteristics: controlling the false positive rate, improving generalized power, and

enabling early termination of arms. These results underscore the potential of the BHARP method to efficiently investigate effect heterogeneity and reduce the cost of clinical trials.

Unlike K-means and Bayesian model averaging, BHARP model adjusts borrowing strength to cohesion within cluster. Compared to Dirichlet process mixture models which assume a potentially unbounded number of components, the BHARP method offers a more transparent and practically intuitive framework for incorporating expert knowledge while maintaining flexibility. In addition, the BHARP method produces model-averaged posterior estimates across plausible TEH structures, enabling coherent uncertainty quantification. Future extensions could explore structured elicitation of prior knowledge about TEH structures.

In addition to its methodological innovations, the BHARP framework provides a practical computational advancement by extending rjMCMC to the context of dynamically partitioning heterogeneous treatment effects. While rjMCMC has been widely used for variable selection, its application to partitioning-based information borrowing has remained largely unexplored, partly due to the challenge of designing reversible moves compatible with the constraints in clinical settings. In particular, under the limited effect sizes and sample sizes typical of clinical trials, poorly constructed transdimensional moves may induce incoherent or misleading partitions. To address this, we adapted the classical split-merge framework [Nobile and Green, 2000] with several domain-specific modifications: an informative prior on the number of components to encourage conservative borrowing, a higher frequency of split proposals to mitigate overmerging, and tuned auxiliary variable distributions to improve the plausibility and acceptance of proposed splitting moves. These enhancements enable the algorithm to explore clinically meaningful partitions and increase its capacity to detect subtle heterogeneity. We provide a C++ implementation with an R interface. This computational development bridges the gap between statistical theory and clinical application and lays the foundation for future extensions of Bayesian partition models.

From a practical standpoint, the proposed method offers a flexible and interpretable tool to incorporate TEH into the design and analysis of clinical trials. For investigators aiming to identify TEH with BHARP model, several design considerations may help improve trial outcomes. First, the interpretability of TEH critically depends on the subgroups prespecified at the design stage. Subgroups defined by meaningful prognostic covariates are more likely to reveal strong TEH, thus supporting treatment decision-making and revealing underlying biological mechanisms, which enhances inferential value without increasing sample size. Subgroup definitions should therefore be guided by clinical knowledge or prior evidence whenever possible. Second, the ability of the BHARP method to detect fine-grained heterogeneity depends on the availability of sufficient information. When the TEH structure is likely subtle, a larger sample size is essential to reliably identify it; otherwise, the model must place greater reliance on informative priors, making prior elicitation and hyperparameter calibration especially critical in low-signal settings. Finally, it is important to recognize that the BHARP model builds its hierarchical structure on subgroup-specific parameters, where the fundamental units of inference and partitioning are subgroups rather than individuals. Consequently, the number and distribution of subgroups play a critical role in the informativeness of data. For a fixed sample size, a more balanced distribution across subgroups typically provides greater inferential resolution than an imbalanced design with highly concentrated observations. When certain subgroups are expected to be underrepresented, investigators may consider stratified randomization or targeted recruitment strategies to ensure adequate sample sizes across all prespecified subgroups, thereby supporting more reliable detection of TEH.

The proposed approach can be extended in several directions. First, this work assumes that subgroups are prespecified based on external criteria. Exploring how to define subgroups from candidate covariates—such as selecting predictive biomarkers or identifying thresholds—is beyond the scope of this paper. Future work could extend the BHARP framework to address continuous covariates by leveraging ideas from Maleyeff et al. [2024], who propose a Bayesian model averaging approach to identify the thresholds defining the subgroups. Integrating such strategies into the BHARP framework enable data-driven threshold identification in multi-arm trials while preserving flexible information borrowing across subgroups. Second, although the proposed approach supports flexible inference of TEH structures, this information is not yet fully incorporated into the decision rules of our trial design. A possible extension is to incorporate posterior measures of certainty into adaptive allocation—for instance, by assigning more resources to complex TEH structures.

## Supplementary Materials

Supplementary Materials are available in the ancillary files of this arXiv submission.

## Acknowledgements

This research was supported by a doctoral scholarship from the Fonds de recherche du Québec – Nature et technologies (FRQNT). SG acknowledges support from the Natural Sciences and Engineering Research Council of Canada (NSERC), Canadian Institute for Statistical Sciences (CANSSI), and Fonds de recherche du Québec - Santé (FRQS) and FRQNT. The authors acknowledge the use of computing resources provided by the Digital Research Alliance of Canada.

## Data availability statement

The code for the proposed method and scripts to reproduce the simulation studies will be available at GitHub repository. Simulation code is available upon request and will be made public upon acceptance.

## References

- Boris Freidlin, Lisa M McShane, and Edward L Korn. Randomized clinical trials with biomarkers: Design issues. *Journal of the National Cancer Institute*, 102(3):152–160, 2010.
- Michael Rosenblum and Daniel F Hanley. Adaptive enrichment designs for stroke clinical trials. *Stroke*, 48(7):2021–2025, 2017.
- Ganggang Xu, Huirong Zhu, and J Jack Lee. Borrowing strength and borrowing index for Bayesian hierarchical models. *Computational statistics & data analysis*, 144:106901, 2020.
- Peter F Thall. Adaptive enrichment designs in clinical trials. *Annual review of statistics and its application*, 8(1):393–411, 2021.
- Peter F Thall, J Kyle Wathen, B Nebiyou Bekele, Richard E Champlin, Laurence H Baker, and Robert S Benjamin. Hierarchical Bayesian approaches to phase II trials in diseases with multiple subtypes. *Statistics in medicine*, 22(5):763–780, 2003.
- Scott M Berry, Kristine R Broglio, Susan Groshen, and Donald A Berry. Bayesian hierarchical modeling of patient subpopulations: Efficient designs of phase II oncology clinical trials. *Clinical Trials*, 10(5):720–734, 2013.
- Nan Chen and J Jack Lee. Bayesian cluster hierarchical model for subgroup borrowing in the design and analysis of basket trials with binary endpoints. *Statistical Methods in Medical Research*, 29(9):2717–2732, 2020.
- Haiyan Zheng and James MS Wason. Borrowing of information across patient subgroups in a basket trial based on distributional discrepancy. *Biostatistics*, 23(1):120–135, 2022.
- Yiyi Chu and Ying Yuan. A Bayesian basket trial design using a calibrated Bayesian hierarchical model. *Clinical Trials*, 15(2):149–158, 2018a.
- Beat Neuenschwander, Simon Wandel, Satrajit Roychoudhury, and Stuart Bailey. Robust exchangeability designs for early phase clinical trials with multiple strata. *Pharmaceutical statistics*, 15(2):123–134, 2016.
- Nan Chen and J Jack Lee. Bayesian hierarchical classification and information sharing for clinical trials with subgroups and binary outcomes. *Biometrical Journal*, 61(5):1219–1231, 2019.
- Liyun Jiang, Ruobing Li, Fangrong Yan, Timothy A. Yap, and Ying Yuan. Shotgun: A Bayesian seamless phase I-II design to accelerate the development of targeted therapies and immunotherapy. *Contemporary Clinical Trials*, 104:106338, 2021. ISSN 1551-7144.
- Daniel Kang, Christopher S Coffey, Brian J Smith, Ying Yuan, Qian Shi, and Jun Yin. Hierarchical Bayesian clustering design of multiple biomarker subgroups (HCOMBS). *Statistics in medicine*, 40(12):2893–2921, 2021.
- Tianjian Zhou and Yuan Ji. Bayesian methods for information borrowing in basket trials: An overview. *Cancers*, 16(2):251, 2024.
- Xuetao Lu and J Jack Lee. Overlapping indices for dynamic information borrowing in Bayesian hierarchical modeling. *arXiv preprint arXiv:2305.17515*, 2023.
- Matthew A Psioda, Jiawei Xu, QI Jiang, Chunlei Ke, Zhao Yang, and Joseph G Ibrahim. Bayesian adaptive basket trial design using model averaging. *Biostatistics*, 22(1):19–34, 2021.
- Brent R Logan, Rodney Sparapani, Robert E McCulloch, and Purushottam W Laud. Decision making and uncertainty quantification for individualized treatments using bayesian additive regression trees. *Statistical methods in medical research*, 28(4):1079–1093, 2019.
- Peter J Green. Reversible jump Markov chain Monte Carlo computation and Bayesian model determination. *Biometrika*, 82(4):711–732, 1995.

- Agostino Nobile and Peter J Green. Bayesian analysis of factorial experiments by mixture modelling. *Biometrika*, 87(1):15–35, 2000.
- Yiyi Chu and Ying Yuan. BLAST: Bayesian latent subgroup design for basket trials accounting for patient heterogeneity. *Journal of the Royal Statistical Society Series C: Applied Statistics*, 67(3):723–740, 2018b.
- Hugh A. Chipman, Edward I. George, and Robert E. McCulloch. BART: Bayesian additive regression trees. *The Annals of Applied Statistics*, 4(1):266–298, March 2010.
- Lara Maleyeff, Shirin Golchi, Erica EM Moodie, and Marie Hudson. An adaptive enrichment design using bayesian model averaging for selection and threshold-identification of predictive variables. *Biometrics*, 80(4):uiae141, 2024.